physica status solidi

pss

www.pss-journals.com

reprint

WILEY-VCH

Phys. Status Solidi RRL **8**, No. 7, 639–642 (2014) / **DOI** 10.1002/pssr.201409148

pss +++rapid research letters+++
www.pss-rapid.com

Room-temperature photoluminescence in quasi-2D $TlGaSe_2$ and $TlInS_2$ semiconductors

Vytautas Grivickas[*,1], Karolis Gulbinas[1], Vladimir Gavryushin[1], Vitalijus Bikbajevas[1], Olga V. Korolik[2], Alexander V. Mazanik[2], and Alexander K. Fedotov[2]

[1] Institute of Applied Research, Vilnius University, Sauletekio av. 10, 10223 Vilnius, Lithuania
[2] Department of Energy Physics, Belarusian State University, 220030 Minsk, Belarus

Received 1 April 2014, revised 7 May 2014, accepted 20 May 2014
Published online 28 May 2014

Keywords thallium dichalcogenides, photoluminescence, optical absorption, anisotropy

[*] Corresponding author: e-mail vytautas.grivickas@ff.vu.lt, Phone: +370 614 45311

We reveal the intrinsic band-to-band photoluminescence (PL) in Tl-based anisotropic semiconductors by means of confocal spectroscopy. The PL achieves largest value for $\boldsymbol{k} \perp \boldsymbol{c}$, where $\boldsymbol{c}$ is the layers stacking axis, and is dependent on polarization. In $TlGaSe_2$, the band edge absorption spectra were determined at different excitation geometry by using techniques of depth-resolved free-carrier absorption (FCA) and photoacoustic response (PAR). A strong absorption enhancement is detected in a large spectral area in the near-surface region lateral to *ab* plane. The band-to-band absorption enhancement is the most probable cause for high PL intensity. The near-surface behavior, different from the bulk, might implement useful photonic functionality at room temperature (RT).

1 Introduction The Tl dichalcogenides $TlMX_2$ (metal M = Ga, In, chalcogen X = Se, S) with naturally 2D-layered structure undergoing sequential phase transitions below RT received a great attention for applications in optoelectronics [1–6]. Their crystal structures belong to the monoclinic symmetry group $C_c^2 - C_{2h}^6$ with crystallographic c^*-axis which has a small ~10° deviation from a normal to the (001) *ab* plane *c*-axis. The atomic arrangement is shown in the inset of Fig. 1. The layers are composed of dense M_4X_{10} polyhedra representing a corner-connected MX_4 tetrahedron. The unit cell of the crystal is made of two layers twisted by 90°. The interlayer bonding between Tl and X atoms is weak. It sustains on buried Tl^+ atom positioned in lines along $\boldsymbol{a}$ [110] or $\boldsymbol{b}$ [$1\bar{1}0$] directions, parallel to the edges of M_4X_{10}. For this reason, the crystal exhibits a distinct anisotropy which clearly manifests in the mechanical properties, an easy cleavage of layers parallel to the *ab* plane and termination of their edges along the $\boldsymbol{a}$, $\boldsymbol{b}$ directions.

In the past, a number of optical spectroscopy studies have been performed using these semiconductors under a convenient light direction normal to the *ab* plane; $\boldsymbol{k} \parallel \boldsymbol{c}$, $\boldsymbol{E} \perp \boldsymbol{c}$. These studies revealed predominantly forbidden electron transitions and a close indirect and direct optical band gaps resulting from the weak covalent nature of the interlayer bonding [2–9]. In agreement with theoretical calculations of the electronic structure [6, 9, 10], the restriction of the band gap optical transitions comes from the fact that the bottom of the conduction band is mainly composed of Tl:6p orbitals whereas the top of the valence band of X:4p orbitals. The amount of states which symmetry forbids the transition in the dipole approximation is vastly larger in $TlGaSe_2$ than in $TlInS_2$. That is confirmed by optical band-to-band absorption value measured around the lowest direct Γ-exciton at RT: in $TlGaSe_2$, $\alpha_{bb} \approx 1 \times 10^2$ cm^{-3}, $E_{ex}^d = 2.09$ eV [7, 8] and in $TlInS_2$, $\alpha_{bb} \approx 1.4 \times 10^3$ cm^{-3}, $E_{ex}^d = 2.44$ eV [2]. According to the detailed balance principle weak absorption gives rise to slight emission. Actually, the intrinsic PL obtained by conventional technique was observed at $T < 2.2$ K in $TlGaSe_2$ [11] and at $T < 20$ K in $TlInS_2$ [12] when both materials reside in the ferroelectric F-phase. Only rather recently the PL at RT achieved by confocal spectroscopy was presented in [13].

For light direction parallel to the layers ($\boldsymbol{k} \perp \boldsymbol{c}$), one might expect more allowed transition in the $\boldsymbol{E} \parallel \boldsymbol{c}$ orientation as exposed in GaSe layered semiconductor [1]. The optical data in $TlMX_2$ were extracted from the $\boldsymbol{E} \parallel \boldsymbol{c}$ component at oblique incidence to *ab* plane. The dielectric function, band gap energy, birefringence, and Γ-exciton energy were estimated under the assumption of a uniaxial anisotropy with respect to the *c*-axis [2, 14]. However, absorption data for $\boldsymbol{E} \parallel \boldsymbol{c}$ near the band gap remain controversial, the polarization dependencies were not determined.

We report results of the intrinsic PL and its polarization dependence obtained by the confocal PL microscopy for both $\boldsymbol{k} \perp \boldsymbol{c}$ and $\boldsymbol{k} \parallel \boldsymbol{c}$ illumination directions at RT. To account for these features, a combining study of light absorption in $TlGaSe_2$ by FCA and PAR dynamic techniques has been carried out by excitation from specular lateral faces. (It must be noted, that the preparation of samples with specular faces vertical to the *ab* plane turned out to be a difficult task.) Such approach allowed us to ascertain the existence of the near-surface region on the lateral crystal edges, not accounted before, which has substantially different optoelectronic property than in the bulk of the 2D-structures.

2 Experimental details The explored samples were grown by the Bridgman method from stoichiometric compositions of a melt; the element ratio was identified by energy-dispersive X-ray spectroscopy. We investigated a single undoped β-$TlInS_2$ and nine batches of $TlGaSe_2$; five of which were initially undoped and four doped with Fe, Tb, B and Al by adding elements into the melt in the amount of 0.1–0.5%. The samples were reduced into the small pieces of the required parallelepiped oriented along *ab*, *ac*, *bc* surfaces. Two thicker undoped $TlGaSe_2$ plates for FCA and PAR study were produced by gentle polishing their lateral surfaces to optical quality, with a following removal of damaged crystal layers by cleavage. These procedures allowed forming rectangular corners of the sample (Fig. 1).

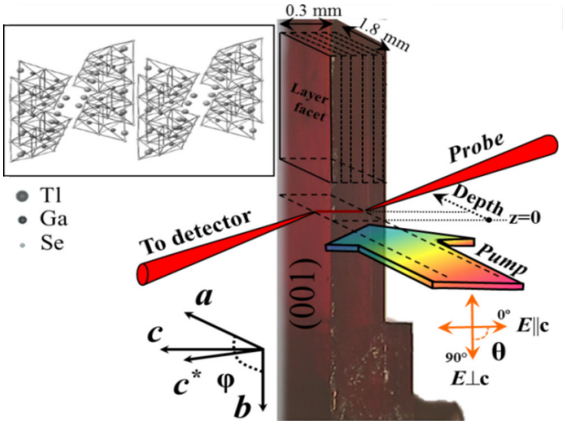

Figure 1 Sample and schematics of FCA and PAR measurement at $\boldsymbol{k} \perp \boldsymbol{c}$ pump direction. The inset shows the atomic structure of the layered $TlGaSe_2$ crystal.

The PL and Raman measurements were performed in the backscattering geometry by Nanofinder HE (LOTIS TII Belarus, Japan) apparatus with a confocal 3D-scanning microscope with 0.95 numerical aperture achieving a large collection angle of emitted light from a nearly uniform segment on the selected surface [15], and a 0.02 nm resolution spectrometer equipped with a cooled CCD camera. The excitation was performed by linearly polarized light of cw-laser at 532 nm, 473 nm or 405 nm wavelength. In most cases, the diameter of the spot was about 200 nm. Most of the data were taken with an excitation power of 60 μW which is 2–6 times lower than of the estimated power resulting in the irreversible degradation.

The FCA and PAR measurements were performed using perpendicular configuration of pulsed-pump and cw-probe beams, as illustrated in Fig. 1 by an appropriate scheme for the $\boldsymbol{k} \perp \boldsymbol{c}$ pump direction. The excitation was provided by a 1 ns rise-time tunable wavelength YAG laser operating at the repetition of 40 Hz; a linear polarization is maintained (rotated) by a Barek polarizer. The illumination spot was of about 0.9 mm in diameter. The tightly focused (~8 μm) infrared cw-light of 1540 nm was emitted from the 20 mW LED. The beam is aligned precisely parallel to the illuminated facet. The sample is mounted on a translation stage that allows a motorized scan in *z*-direction with 1 μm precision. Further details of experimental set-up are given in Refs. [4, 16]. The light-induced FCA ($\Delta\alpha$) amplitude is related to the injected carriers concentration (Δp): $\Delta\alpha = \sigma_{eh}\Delta p$, where σ_{eh} is the electron–hole pair absorption cross-section. At a time immediately after pump pulse, the depth profile of free carriers is consistent with the extinction of local intensity I_{ex}, i.e. $\Delta p(z) = \Delta p(0) \exp(-\alpha_{bb} \cdot z)$, where z is measured from the illuminated surface and $\Delta p(0) = (1 - R)\, I_{ex}(0)\, \alpha_{bb}(0)/(\hbar\omega)$, where R is the reflectivity and $\hbar\omega$ is the quantum energy. This relation was used for obtaining α_{bb} spectrum near the illuminated surface for α_{bb} value below 3×10^3 cm^{-1} using the procedures described in Ref. [16]. The PAR was monitored at a distance $z = 300$ μm from the illuminated surface. The photoacoustic stress is at a level of several milibars. The PAR is directly related to the longitudinal acoustic wave travelling in the crystal and inducing a temporal pressure change of the refractive index which is monitored via probe beam deflection. A knife edge measurement of the probe beam allows to detect a small variation of the refractive index; further details are described in Ref. [4]. The refractive index is proportional to the absorbed energy near the free surface due to the electron–phonon acoustic deformation mechanism.

3 Results and discussion Figure 2 shows the PL spectra after excitation with polarized light of 2.62 eV and 2.33 eV quantum energy in $TlInS_2$ and $TlGaSe_2$, respectively. The intralayer optical phonon accompanied Raman lines appear below these excitation energies. The Raman lines virtually are independent of the exciting light polarization. The observed PL spectra are wide Gaussian curves;

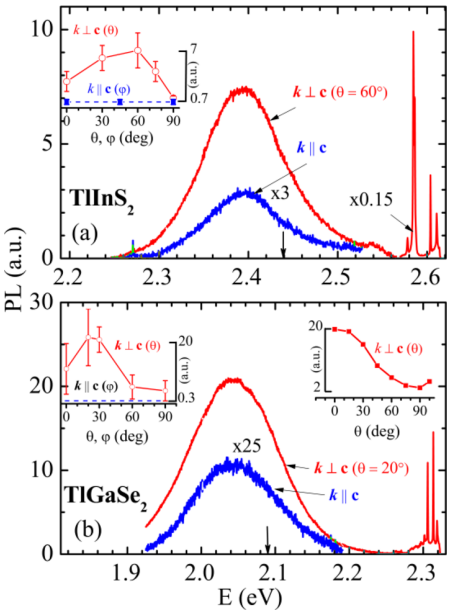

Figure 2 PL and Raman lines obtained from *ab* plane (blue) and from lateral surfaces (red): (a) in $TlInS_2$ ($h\nu_{exc} = 2.62$ eV) and (b) in undoped $TlGaSe_2$ ($h\nu_{exc} = 2.33$ eV). The left insets show the PL peak as a function of excitation light polarization (angles θ, φ are shown in Fig. 1) for a constant excitation power; the error bar represents statistical spread of the results from different spots in the same sample. The right inset in (b) shows the polarization dependence of PL light after 3.06 eV excitation ($\boldsymbol{k} \perp \boldsymbol{c}$).

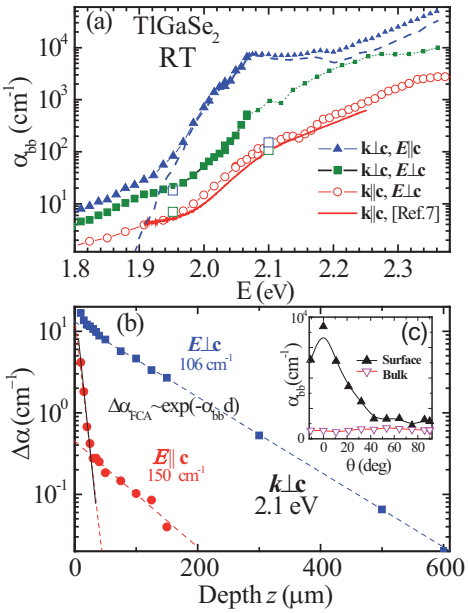

Figure 3 (a) Absorption spectra in $TlGaSe_2$ at different excitation geometry obtained from FCA – large symbol and PAR – small symbol. Open squares: measurement in the bulk for ($\boldsymbol{k} \perp \boldsymbol{c}$). Solid line conventional measurement [7]. Direct absorption given by the dashed line was used for PL simulation. (b) Light-induced depth distribution of FCA at $\boldsymbol{k} \perp \boldsymbol{c}$, extracted α_{bb} values are indicated. (c) Polarization dependences of the absorption in the near-surface region and in the bulk at 2.1 eV.

the PL peaks appear below the Γ-exciton energies [2, 8] as indicated by vertical arrows. The PL nearly linearly increases with the excitation power and is not detected for excitation quanta below the band gap. These peculiarities are typical for the intrinsic band-to-band emission mechanism. The fit parameters of PL spectra are given in Table 1. A variation in the fit parameters in samples from different batches of $TlGaSe_2$ implies some influence on the intrinsic PL mechanism from a possible variation of the most common defect in the layered crystals, the stacking faults. As shown by the dashed line in the left inset of Fig. 2, the PL peak, however, is independent of excitation polarization (φ angle) or the spot position for measurement in the *ab* plane. However, the PL for $\boldsymbol{k} \perp \boldsymbol{c}$ substantially varies with the measured spot position in the same sample as represented by error bars. Moreover, for $\boldsymbol{k} \perp \boldsymbol{c}$ the PL exhibits polarization dependence contrary to the $\boldsymbol{k} \parallel \boldsymbol{c}$ and also experiences a strong enhancement as compared with $\boldsymbol{k} \parallel \boldsymbol{c}$ case. The enhancement factor is as much as 7 for $\theta \approx 60°$ in $TlInS_2$ and ≥50 for $\theta \approx 20°$ in $TlGaSe_2$. The PL after convenient excitation $\boldsymbol{k} \parallel \boldsymbol{c}$ was noticed only in one undoped $TlGaSe_2$ sample. No observable PL was detected in $TlGaSe_2$ sample batches doped with Ag and Fe. The latter fact can be attributed to an overlapping of absorption edge with the impurity absorption bands related to these dopants. This feature was explicitly proven in $TlGaSe_2$:Fe [8]. The right inset in Fig. 2b shows PL light polarization obtained after 3.06 eV excitation. The sinusoidal dependence of the PL light approaches a maximum at $\boldsymbol{E} \parallel \boldsymbol{c}$ ($\theta = 0$). The obtained feature testifies that in $TlGaSe_2$ the PL emission is associated with excitations of out-of-plane oriented dipoles.

Table 1 Fitting parameters of the Gaussian shape PL spectra.

semiconductor	PL peak (eV)	FWHM (eV)
$TlGaSe_2^*$	2.042 ± 0.01	0.142 ± 0.04
$TlInS_2$	2.395	0.11

* The error bars account for the variation of the PL among five undoped batches and two batches of the samples doped with 0.1% of Al and B.

The α_{bb} absorption spectra in $TlGaSe_2$ for two illumination directions are presented in Fig. 3a. In the case of normal light incidence ($\boldsymbol{k} \parallel \boldsymbol{c}$, $\boldsymbol{E} \perp \boldsymbol{c}$), α_{bb} obtained from the FCA is shown by open circles, and does almost coincide with the unpolarized spectrum obtained by conventional optical transmission (solid red line) [7]. No polarization dependence in this case was detected. For illumination through the lateral facet ($\boldsymbol{k} \perp \boldsymbol{c}$), an enhanced absorption was found. The enhancement is detected in the large spectral area around the band gap. It can be estimated from Fig. 3a how many times the PL is enhanced. Namely, for $\boldsymbol{E} \perp \boldsymbol{c}$: 4 times (at 1.9 eV), 4 (2.0 eV) and 7 (2.1 eV) and far more for $\boldsymbol{E} \parallel \boldsymbol{c}$: 8 (1.9 eV), 47 (2.0 eV), 100 (2.1 eV). Such enhancement is really surprising since it testifies that not only the Γ-direct absorption becomes allowed, as ex-

pected, but also the indirect and the sub-band gap absorption increases as well. Furthermore, the FCA data indicate that the enhanced absorption does not remain the same in the bulk of the sample. This is disclosed in Fig. 3b by depth-distribution measurement of FCA for $\boldsymbol{k} \perp \boldsymbol{c}$ at 2.1 eV energy corresponding to Γ-exciton. The strong absorption reflected by high slope of $\exp(-\alpha_{bb} \cdot z)$ persists to about 40 μm. The α_{bb} in this region obeys a dependence on angle θ with a maximum at $\theta = 0$ ($\boldsymbol{E} \parallel \boldsymbol{c}$, Fig. 3c, solid triangles). In the bulk region ($z > 40$ μm), the α_{bb} is substantially lower: $\alpha_{bb} = 106\ cm^{-1}$ ($\boldsymbol{E} \perp \boldsymbol{c}$) and $150\ cm^{-1}$ ($\boldsymbol{E} \parallel \boldsymbol{c}$). These values are very close to those measured for illumination normal to *ab* plane ($\boldsymbol{k} \parallel \boldsymbol{c}$), as shown in Fig. 3a by large open squares. Moreover, the polarization dependence of α_{bb} in the bulk is almost negligible; see Fig. 3c, open triangles. Thus, we conclude that enhancement is most probably caused by particular material property which exists in the near-surface region. By performing the depth-resolved FCA measurement for excitation from different lateral surfaces in two polished $TlGaSe_2$ samples the thickness variation of near-surface region was estimated to be 30–100 μm. It seems likely that the variation in the depth of near-surface region for broken lateral surface is larger than for polished one, as evidenced by large fluctuations of the intrinsic PL, see Fig. 2, left insets. The near-surface region depth of broken lateral surfaces is expected to be not less than a few micrometers.

Hence, we assume that during the process of crystal polishing (or breaking) the structural crumpling of the crystal unit cell takes place all along the surface which leads to small variations between the bonding angles of corner-connected M_4X_{10} polyhedron units. That, in its turn, acts on the weak coupling of the buried interlayer Tl–X bonds (see inset to Fig. 1) and results in a modification of the states at the extrema of the bands. The validation of slippage ability of Tl^+ ion along to ***a***, ***b***-direction or to both was proven theoretically [17]. It was assumed that after slippage, Tl^+ ion interaction is causing Tl:6p and Tl:6s orbital mixing. Currently, this property is the most common explanation for the occurrence of the easy F-phase transition in Tl-based 2D-semiconductors at low temperature [1, 3–5, 8].

The presented data imply that the PL in $TlGaSe_2$ (and in $TlInS_2$ as well) at RT can be explained by two main contributions. The first is simply the injected carrier density which is proportional to polarization dependent absorption at the excitation energy. The second one, according to the detailed balance principle, is proportional to the enhanced absorption, resulting from transition between states close to the extremum of valence and conductive bands. This contribution determines the shape of the PL and is independent of the first one. We have performed the preliminary PL spectra simulation in $TlGaSe_2$ based on the detailed balance principle and using the direct band-to-band absorption from the spectrum obtained at $\boldsymbol{k} \perp \boldsymbol{c}$, $\boldsymbol{E} \parallel \boldsymbol{c}$, shown in Fig. 3a by the dashed line. (The details will be presented elsewhere.) The ground state 2.095 eV Γ-exciton and the direct band gap $E_g = 2.12$ eV, both broadened by 35 meV, were applied for the PL simulation. We were able to reproduce the experimentally measured PL spectrum shape in the case of dipole-forbidden optical transition as well as for the dipole-allowed one. As a matter of fact, the oscillator strength of the dipole-allowed optical transitions from the ground state of the exciton was essential to be reduced by 100 times. Further investigations at low T may furnish more insights into the nature of exciton transitions and phonon contribution to the PL spectrum. Therefore, existing of RT PL in quasi-2D-semiconductor structure possesses the ability to fabricate a polarization sensitive device operating at RT.

Acknowledgements This study was supported by Swedish Visby program project No. 00729.

References

[1] A. M. Panich, J. Phys.: Condens. Matter. **20**, 293202 (2008).
[2] Y. Shim, Y. Nishimoto, W. Okada, K. Wakita, and N. Mamedov, Phys. Status Solidi C **5**, 1121 (2008).
[3] M. Yu. Seyidov, R. A. Suleymanov, and E. Yakar, J. Appl. Phys. **106**, 023532 (2009).
[4] V. Grivickas, V. Bikbajevas, V. Gavryushin, and J. Linnros, J. Phys.: Conf. Ser. **100**, 042007 (2008).
[5] M. Yu. Seyidov, R. A. Suleymanov, and F. Salehli, Phys. Lett. A **376**, 643 (2012).
[6] S. Johnsen, Z. Liu, J. A. Peters, J.-H. Song, S. C. Peter, C. D. Malliakas, N. K. Cho, H. Jin, A. J. Freeman, B. W. Wessels, and M. G. Kanatzidis, Chem. Mater. **23**, 3120 (2011).
[7] V. Grivickas, V. Bikbajevas, and P. Grivickas, Phys. Status Solidi B **243**, R31 (2006).
[8] V. Grivickas, V. Gavryushin, P. Grivickas, A. Galeckas, V. Bikbajevas, and K. Gulbinas, Phys. Status Solidi A **208**, 2186 (2011).
[9] G. Orudzhev, Y. Dhim, K. Wakita, N. Mamedov, S. Jafarova, and F. Hashimzade, Jpn. J. Appl. Phys. **47**, 8182 (2008).
[10] S. Kashida, Y. Yanadori, Y. Otaki, Y. Seki, and A. M. Panich, Phys. Status Solidi A **203**, 2666 (2006).
[11] G. I. Abutalybov, I. K. I. K. Nejmanzade, B. S. Rasbirin, E. J. Salajev, and A. N. Staruchin, Soviet Phys. – Semicond. **20**, 1063 (1986).
[12] A. J. Aoyagi, Y. Maryama, S. Onari, K. R. Allakhverdiev, and E. Bairamova, Jpn. J. Appl. Phys. **32**(Suppl. 3), 754 (1993).
[13] K. Wakita, A. Suzuki, U. Miyamoto, D. Huseynova, Y. G. Shim, N. Mamedov, O. Alekperov, A. Najafov, and T. Mammadov, ICTMC-17, Baku, 2010, Abstract O2-1.
[14] Y. Shim, W. Okada, K. Wakita, and N. Mamedov, J. Appl. Phys. **102**, 083537 (2007).
[15] J. A. Schuller, S. Karaveli, T. Schiros, K. He, S. Yang, I. Kymissis, J. Shan, and R. Zia, Nature Nanotechnol., DOI: 10.1038/NNANO.2013.20 (2013).
[16] P. Grivickas, V. Grivickas, J. Linnros, and A. Galeckas, J. Appl. Phys. **101**, 123521 (2007).
[17] K. A. Yee and Th. A. Albright, J. Amer. Chem. Soc. **113**, 6474 (1991).

